AFRL-PR-WP-TR-2003-2051

THERMAL MANAGEMENT RESEARCH FOR POWER GENERATION
Delivery Order 0002 - Volume 1: Plain Fin Array Cooler for Electronics Cooling

Lanchao Lin, Ph.D.

UES, Inc
4401 Dayton-Xenia Road
Dayton, OH 45432-1894

DECEMBER 2002

Final Report for 01 April 2000 – 30 October 2002

**PROPULSION DIRECTORATE
AIR FORCE RESEARCH LABORATORY
AIR FORCE MATERIEL COMMAND
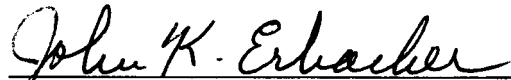WRIGHT-PATTERSON AIR FORCE BASE, OH 45433-7251**

NOTICE

USING GOVERNMENT DRAWINGS, SPECIFICATIONS, OR OTHER DATA INCLUDED IN THIS DOCUMENT FOR ANY PURPOSE OTHER THAN GOVERNMENT PROCUREMENT DOES NOT IN ANY WAY OBLIGATE THE US GOVERNMENT. THE FACT THAT THE GOVERNMENT FORMULATED OR SUPPLIED THE DRAWINGS, SPECIFICATIONS, OR OTHER DATA DOES NOT LICENSE THE HOLDER OR ANY OTHER PERSON OR CORPORATION; OR CONVEY ANY RIGHTS OR PERMISSION TO MANUFACTURE, USE, OR SELL ANY PATENTED INVENTION THAT MAY RELATE TO THEM.

THIS REPORT IS RELEASABLE TO THE NATIONAL TECHNICAL INFORMATION SERVICE (NTIS). AT NTIS, IT WILL BE AVAILABLE TO THE GENERAL PUBLIC, INCLUDING FOREIGN NATIONS.

THIS TECHNICAL REPORT HAS BEEN REVIEWED AND IS APPROVED FOR PUBLICATION.

RENGASAMY PONNAPPAN
Senior Mechanical Engineer
Energy Storage & Thermal Sciences Branch

JOHN K. ERBACHER
Acting Branch Chief
Energy Storage & Thermal Sciences Branch

C. SCOTT RUBERTUS
Acting Deputy Chief
Power Division

Do not return copies of this report unless contractual obligations or notice on a specific document requires its return.

REPORT DOCUMENTATION PAGE			

1. REPORT DATE *(DD-MM-YY)* December 2002	2. REPORT TYPE Final	3. DATES COVERED *(From - To)* 04/01/2000 – 10/30/2002	

4. TITLE AND SUBTITLE
THERMAL MANAGEMENT RESEARCH FOR POWER GENERATION
Delivery Order 0002 - Volume 1: Plain Fin Array Cooler for Electronics Cooling

5a. CONTRACT NUMBER
F33615-98-D-2867

5b. GRANT NUMBER

5c. PROGRAM ELEMENT NUMBER
62203F

6. AUTHOR(S)
Lanchao Lin, Ph.D.

5d. PROJECT NUMBER
3145

5e. TASK NUMBER
32

5f. WORK UNIT NUMBER
Z3

7. PERFORMING ORGANIZATION NAME(S) AND ADDRESS(ES)

UES, Inc
4401 Dayton-Xenia Road
Dayton, OH 45432-1894

8. PERFORMING ORGANIZATION REPORT NUMBER

UES-P183-03-602

9. SPONSORING/MONITORING AGENCY NAME(S) AND ADDRESS(ES)
Propulsion Directorate
Air Force Research Laboratory
Air Force Materiel Command
Wright-Patterson Air Force Base, OH 45433-7251

10. SPONSORING/MONITORING AGENCY ACRONYM(S)
AFRL/PRPS

11. SPONSORING/MONITORING AGENCY REPORT NUMBER(S)
AFRL-PR-WP-TR-2003-2051

12. DISTRIBUTION/AVAILABILITY STATEMENT
Approved for public release; distribution is unlimited.

13. SUPPLEMENTARY NOTES
Report contains color. See also AFRL-PR-WP-TR-2003-2052, Volume 2: Closed-Loop Spray Cooling of High-Power Semiconductor Lasers.

14. ABSTRACT

A fin array cooler was developed to cool a substrate of high-heat flux electronics. Plain copper fin strips were soldered onto the substrate to minimize the contact thermal resistance between the electronics and heat sink. Two new types of fin arrays based on offset fin strips and aligned fin strips were employed in order to mitigate the thermal stress problem found in the integral finned substrate concept. The cooler with different fin strip layouts was tested using polyalphaolefin as the coolant for flow Reynolds number variation from 53 to 482. The fin strip gaps of 0.13, 0.38, and 1.0 mm were experimented. Heat transfer data for different fin strip layouts were obtained under various operating conditions and compared. It was shown that, in general, the heat transfer coefficient was 29 to 36 percent higher for the offset fin strip layout than for the aligned fin strip layout. New heat transfer correlations for offset fin strip layout and aligned fin strip layout are presented.

15. SUBJECT TERMS
electronics cooling, plain fin, offset fin, heat transfer enhancement, heat transfer coefficient, thermal stress

16. SECURITY CLASSIFICATION OF:			17. LIMITATION OF ABSTRACT: SAR	18. NUMBER OF PAGES 38	19a. NAME OF RESPONSIBLE PERSON (Monitor) Rengasamy Ponnappan
a. REPORT Unclassified	b. ABSTRACT Unclassified	c. THIS PAGE Unclassified			19b. TELEPHONE NUMBER *(Include Area Code)* (937) 255-2922

TABLE OF CONTENTS

LIST OF FIGURES

LIST OF TABLES

v

NOMENCLATURE

a   height of a rectangular duct

A_b exposed base surface area

A_c fin cross-sectional area

A_h heating area

b   width of a rectangular duct

c_p constant pressure specific heat

D_h hydraulic diameter, $2ab/(a+b)$

h   heat transfer coefficient

k   thermal conductivity

l   fin length in flow direction

l_{eff} effective fin strip gap

l_g fin strip gap

l_1 effective fin height

m   mass flow rate

n_f number of fins per fin strip

n_{st} number of fin strips

Nu   Nusselt number, hD_h/k_l

p   pressure

P   fin perimeter

Pr   Prandtl number, mc_p/k_l

q   heat flux

Q   heat rate

Re   Reynolds number, ruD_h/m

t   thickness, for fin if no subscript s

T   temperature

u   bulk velocity

μ   fluid dynamic viscosity

ρ density

Subscripts

b   fin base

f   fin

i   inlet

l   coolant

m   mean

o   outlet

s   substrate

FOREWORD

1   INTRODUCTION

One of many commonly used methods of cooling power electronic devices on board aircraft is liquid convection heat transfer by employing polyalphaolefin (PAO) as the circulating coolant. A cooling device of this type that caught our attention at Air Force Research Laboratory (AFRL) includes a dielectric silicon carbide or aluminum compound substrate, a copper fin part soldered onto the dielectric substrate, and a lid with coolant tube manifolds. The dielectric substrate with high thermal conductivity is bonded directly with the die of the electronic components to be cooled. This not only reduces thermal contact resistance but also makes the device compact and reliable. The design issue of the integral dielectric substrate with copper fins mounted onto it becomes critical since two different materials (the dielectric substrate and copper fin) are to be bonded. Thermal stresses due to the mismatch of coefficient of thermal expansion (CTE) could be produced during a fabrication process because of a change in temperature. More specifically, the residual stresses could be generated through a large temperature span between the soldering (or bonding) temperature of the materials (as high as 200°C) and ambient temperature (possibly as low as -40°C).

Under our research program, efforts were made to reduce thermal residual stresses, especially bending moment and peeling stress, in the integral finned substrate as well as to enhance the heat transfer of the cooling device and to minimize the flow pressure drop across the cooling device. As a result, new coolers combining a copper fin array and an aluminum nitride substrate were developed. The fin array consists of a number of plain fin strips and has discrete contact areas on the substrate. The fin strips can be offset or aligned in flow direction and there is a small gap between two consecutive fin strips. With a proper arrangement of the fin strips, the cooler can dissipate the waste heat from the electronic device at levels higher than 40 W/cm^2 with an allowable substrate-to-coolant temperature difference while it still maintains low flow pressure drop (less than 0.02 bar).

The fin array in which any consecutive fin strips are connected in offset arrangement is called the offset strip fin. Numerous researches were done on the offset strip fin [1,2,3]. Manglik and Bergles provided a thorough review of the experimental investigation of offset strip fins [3]. They showed that the only broad-based correlations for offset strip fin compact heat exchangers were those developed by Wieting [4] and 85% of data used by Wieting were correlated to within ±10% for the Colburn j factor, $Nu/(RePr^{1/3})$. Joshi and Webb combined their experimental results with analytical models to

develop correlations for the friction and the Colburn factor in the laminar and turbulent flow regimes and to predict the transition between them [5]. Through flow visualization, they distinguished four different flow regimes. They gave a critical Reynolds number for the laminar-to-turbulent flow transition in terms of the visualization result. DeJong and Jacobi studied the flow and heat transfer in arrays of staggered parallel plates [6]. They made observations of flow through the arrays of the plates and conducted experiments of local, row-by-row and spatially averaged mass transfer. They exhibited a relation between vortex shedding and mass transfer enhancement. Rows in the array where the fins were shedding vortices showed a marked increase in Sherwood number. The vortices were generated at the leading edges of the fins in the unsteady laminar flow regime.

A basic and simple structure related with electronic assemblies is two elastic layers bonded together with an adhesive, as shown in Appendix A. Dissimilar CTEs of both layers and thermal gradients introduce thermal stresses in the layered structure. Numerous studies were undertaken to investigate interlaminar stresses. An effective approach was based on the beam theory that was originally suggested by Timoshenko [7], then refined by Chen and Nelson [8], Suhir [9], and Jiang et al. [10]. This approach was simple and computationally efficient. The present finned substrate could be simplified as the layered structure in order to understand the causes of thermal stresses and find measures of mitigating them.

Little investigation was reported in the literature dealing with heat transfer models of the heat exchanger with discrete plain fin strips (not connected). This paper gives heat transfer characteristics of the new cooler with two types of fin arrays. An empirical heat transfer model is proposed to correlate experimental data of the fin array cooler with various fin strip gaps.

2   PLAIN FIN ARRAYS

Two types of fin arrays were designed and used for test. The fin arrays were made of plain rectangular fin strips with the same size. The cross-sectional view (in flow direction) of the plain fin strip is shown in Figure 2.1. The first type of fin array, denoted as Fin A, is shown in Figure 2.2. In Fin A, the plain fin strips were offset by 0.794 mm from adjacent rows in the flow direction and separated by a gap, l_g. The fin strips were soldered onto the cooling side of the substrate, forming a discrete layout of the contact areas with the dielectric substrate. The second type of fin array, denoted as Fin B, is presented in Figure 2.3. The plain fin strips of Fin B were aligned in the flow direction and also soldered onto the cooling side of the dielectric substrate. On the reverse side of the dielectric substrate, electronic components were mounted. The substrate was made of aluminum nitride (AlN) due to its dielectric and high thermal conductivity feature and was metallized with copper. The thermal conductivity of commonly used AlN was around 170 W/mK. Copper was selected as the fin material since it had a higher thermal conductivity of 393 W/mK. CTE of copper (16.7 ppm/K) was higher than that of AlN (4.6 ppm/K) but lower than CTE values of other common metals with high thermal conductivities (above 100 W/mK). Through the discrete layout of the soldered areas and the folded fin structure across the flow direction, the maximum peeling stress between the fin and substrate and the resultant bending moment exerting on the substrate were noticeably reduced.
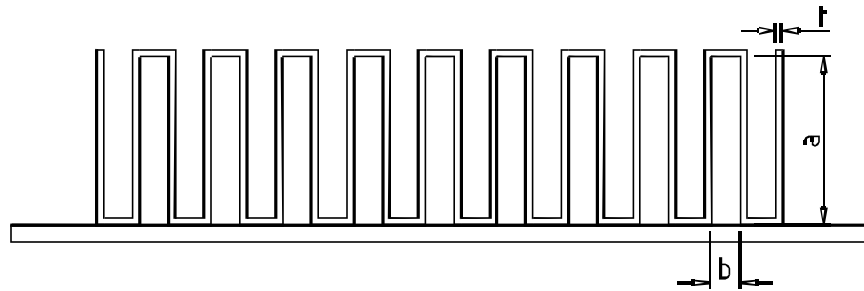
Figure 2.1   Cross-sectional view of the plain fin strip.

3

Plain rectangular copper fin
in offset arrangement

Solder joint

Substrate

Coolant Flow
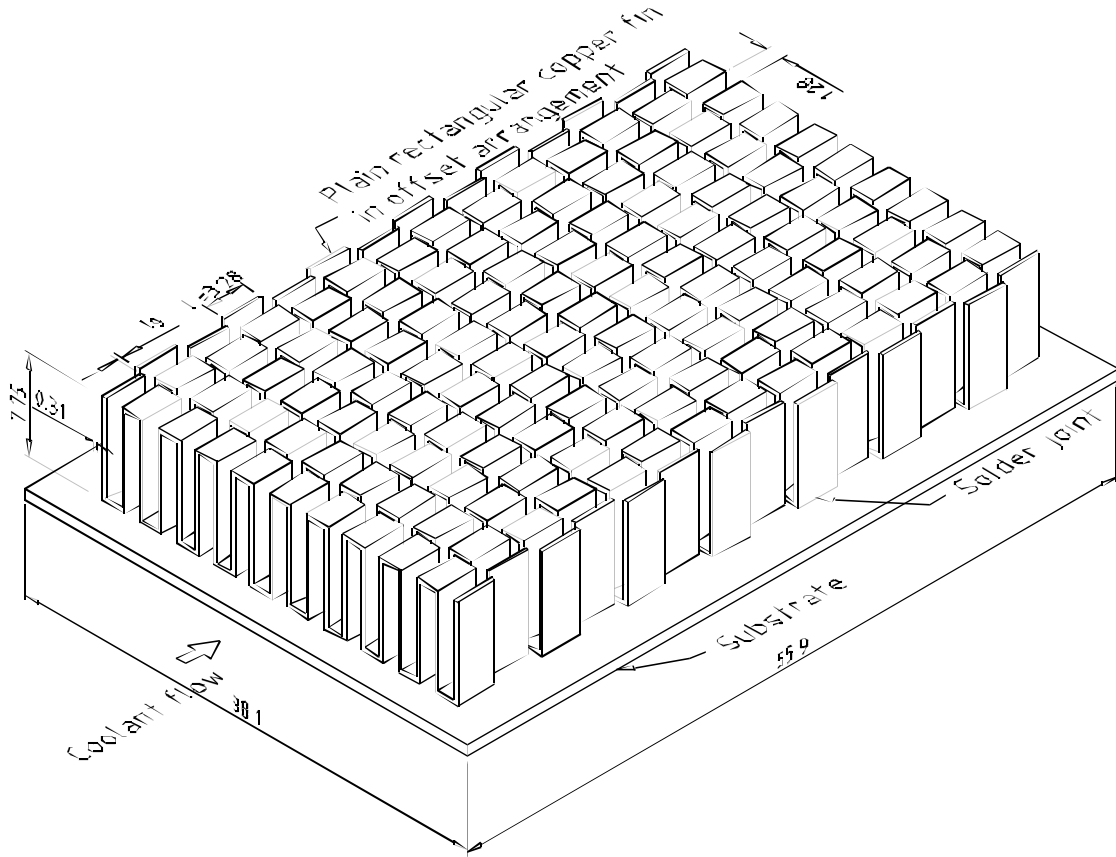
Fin A

Figure 2.2   Plain fin array formed by offset fin strips on the substrate (dimensions in mm).
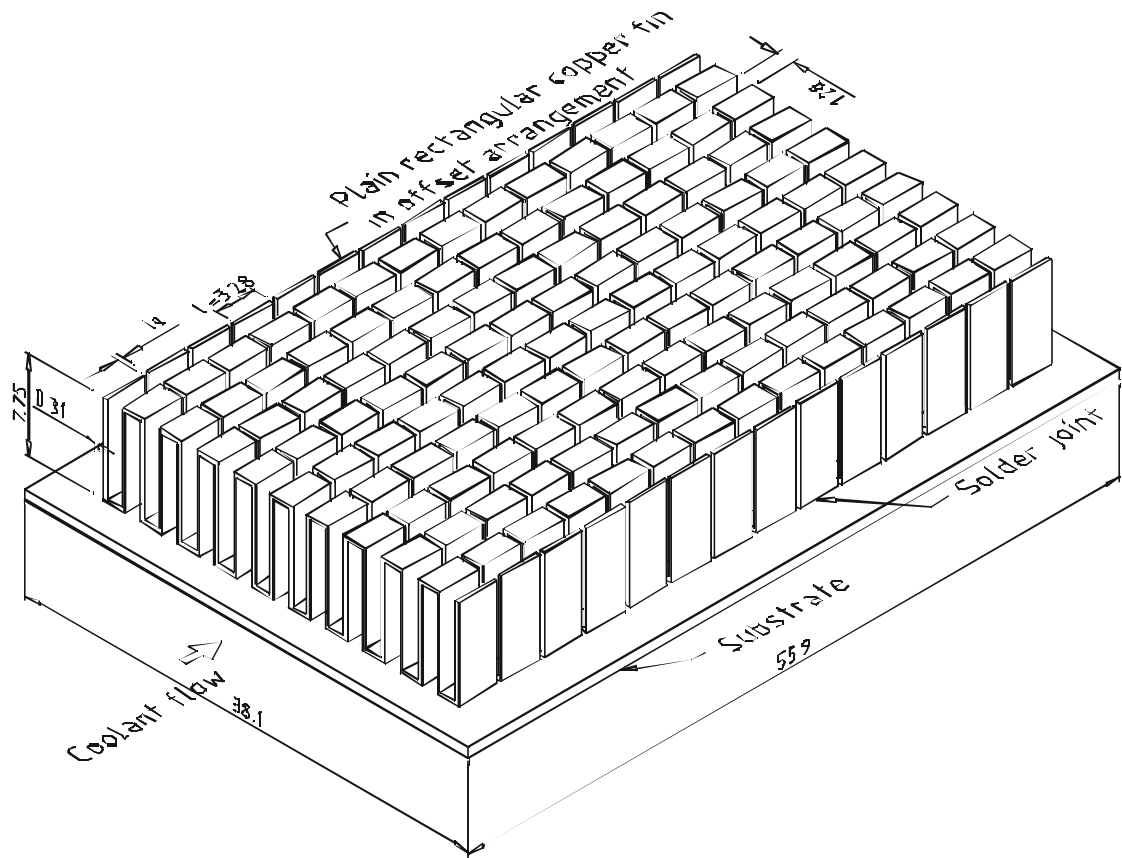
Fin B

Figure 2.3   Plain fin array formed by aligned fin strips on the substrate (dimensions in mm).

Other two high thermal conductivity dielectric materials for the substrate were SiC and Si_3N_4. At present, SiC and AlN are the most widely used ceramics for thermal management of high power electronics. The maximum experimental conductivity of SiC and AlN was about 270 W/mK at room temperature, which presented 50% and 85% of their intrinsic conductivities, respectively. The maximum thermal conductivity of Si_3N_4 was 155 W/mK at room temperature. The high thermal conductivity of Si_3N_4, combined with its excellent mechanical properties, made it a serious candidate as the high reliability substrate. The trend in research on the thermal conductivity of SiC, AlN and Si_3N_4 ceramics was plotted in Figure 2.4 by Watari and Shinde [11]. Key breakthroughs to increase thermal conductivity were also presented in this figure.

Figure 2.4 Trends in the enhancement of the thermal conductivity of SiC, AlN, and Si_3N_4 ceramics during the period 1980 – 2000 [11] and key breakthroughs to increase thermal conductivity.

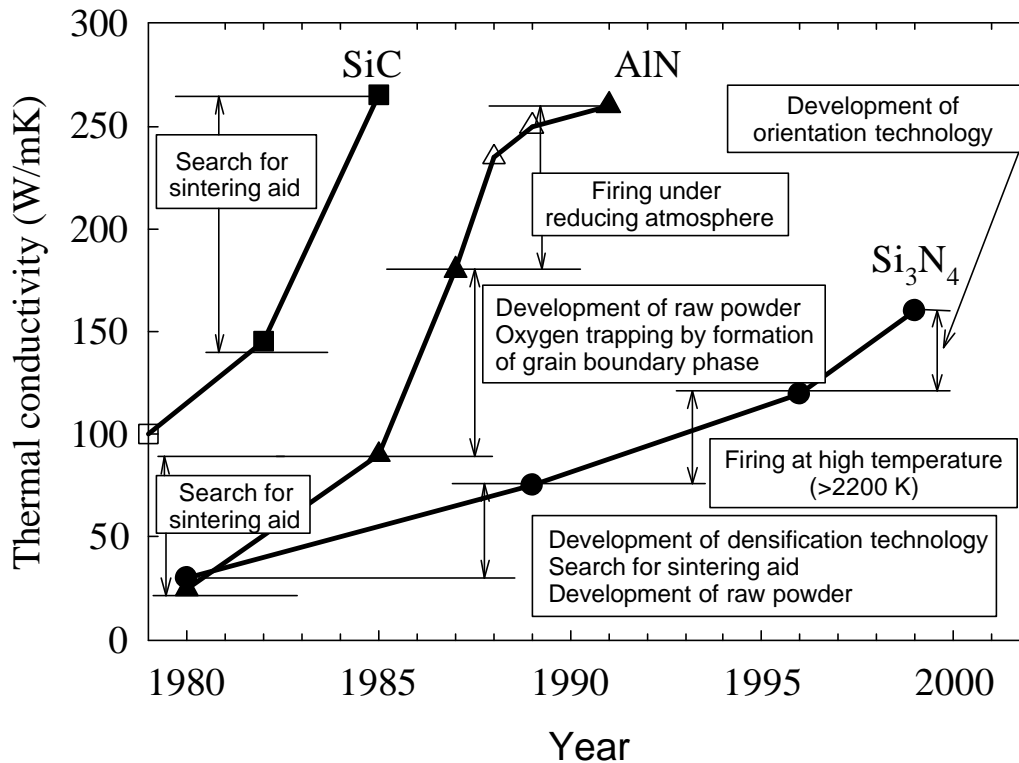The geometric parameters for the two types of the fin arrays are listed in Table 1. The length in flow direction was 3.28 mm which was the minimum fin strip length available in the fin supply market. The fin distance was 1.59 mm/fin. In the group of Fin A type, four fin arrays with the fin strip gaps of 0, 0.13, 0.38 and 1.0 mm were made. In the group of Fin B type, three fin arrays with the fin strip gaps of 0.13, 0.38 and 1.0 mm were made. To reduce the hardware cost, copper plates were used as the substrate for heat transfer test. Figure 2.5 shows the device for mounting the fin array. To make a unitary fin array without noticeably increasing the bending moment on the substrate, the plain fin strips could be connected with expansion turns. This design concept is shown in Appendix B and is not studied in this report.

Table 1　Geometric parameters of plain fin arrays

Parameter	Fin A (offset fin strips)	Fin B (aligned fin strips)
T	0.31 mm	0.31 mm
a	7.44 mm	7.44 mm
b	1.28 mm	1.28 mm
l	3.28 mm	3.28 mm
l_g	0, 0.13, 0.38, 1.0 mm	0.13, 0.38, 1.0 mm
A_h	16.77 cm^2	16.77 cm^2
l_1	8.23 mm	8.23 mm
n_f	20	20
N_{st}	15.5, 15, 14, 12	15, 14, 12
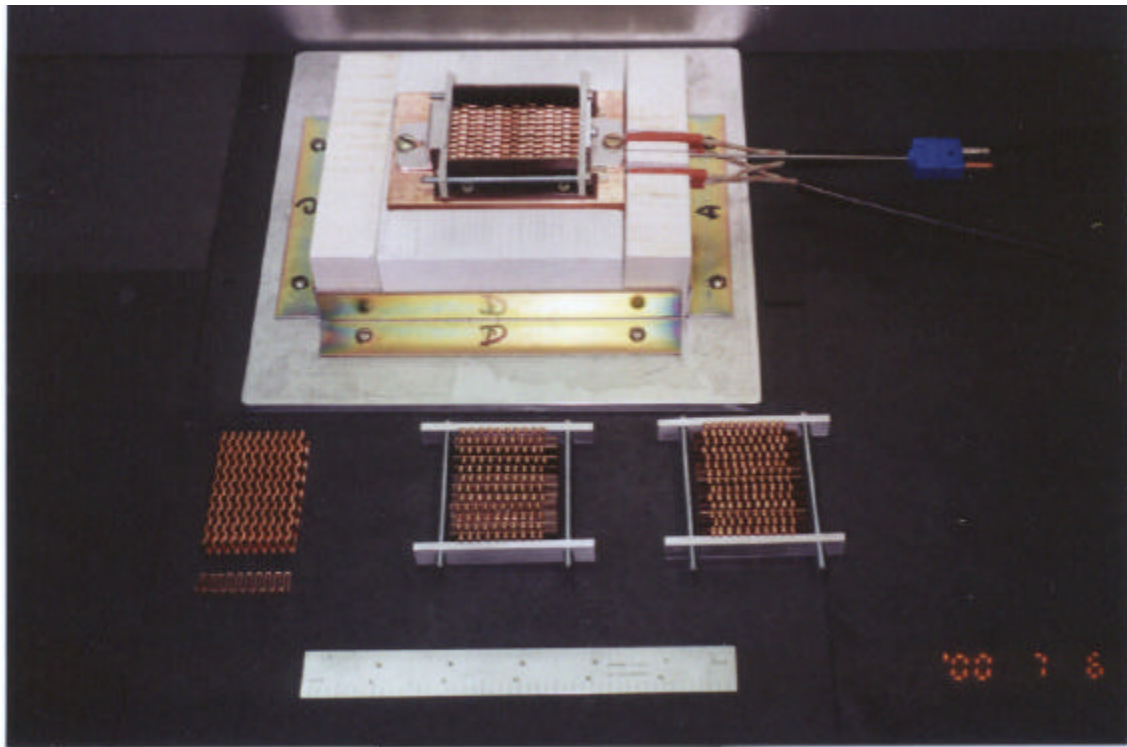
Figure 2.5   Fin array mounting device.

3   EXPERIMENTAL SETUP AND PROCEDURE

The experimental setup was designed for the measurement of heat transfer and pressure drop of the plain fin array cooler. A schematic of the experimental setup is shown in Figure 3.1. A photographic view of the experimental setup is shown in Figure 3.2. The fin array was accommodated in a fin array housing that is shown in Figure 3.3. The coolant flow channel within the cooler was formed by closing a lid onto the top surface of the fin array housing. Two o-rings were used at the contact regions between the fin array housing and the finned substrate and between the fin array housing and the lid. The height and width of the cooling channel were 8.6 mm and 33.78 mm.

Figure 3.1   Schematic of experimental setup.

9
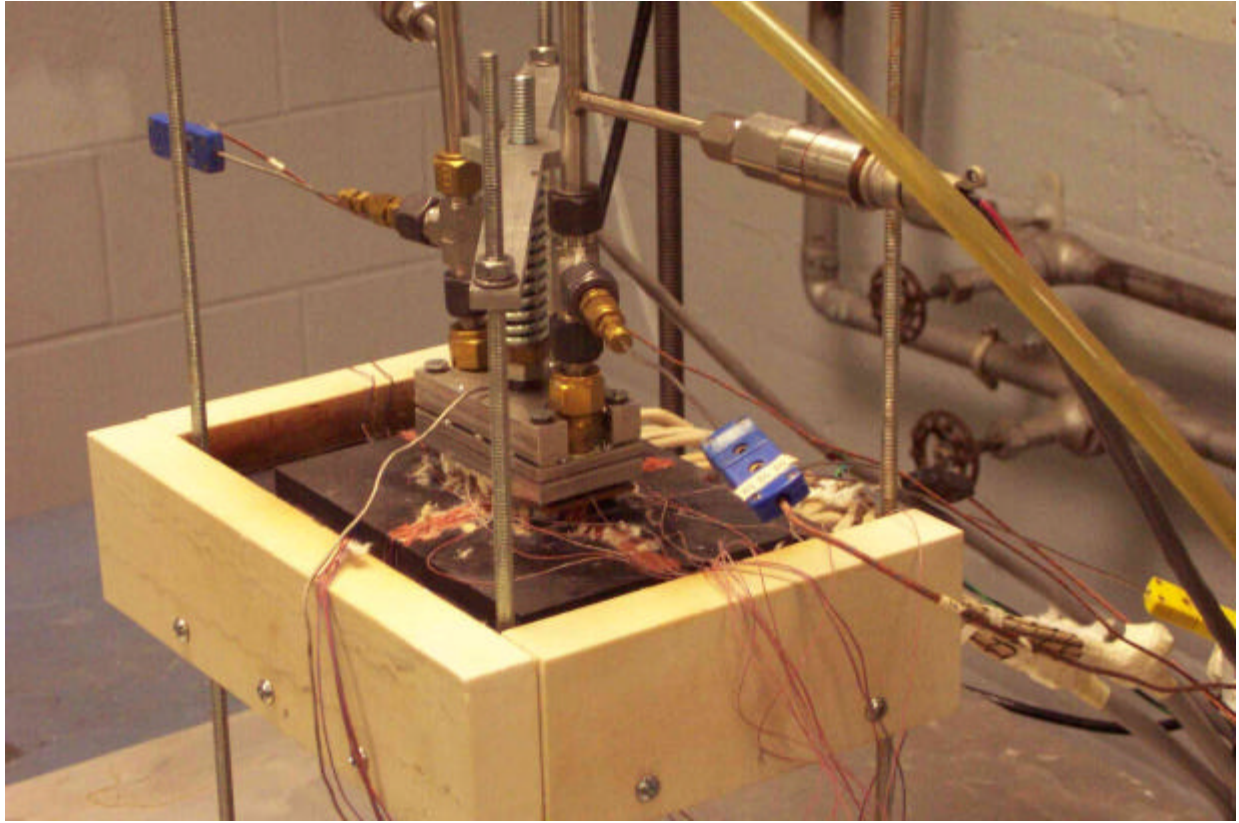
Figure 3.2   Photographic view of the experimental setup.
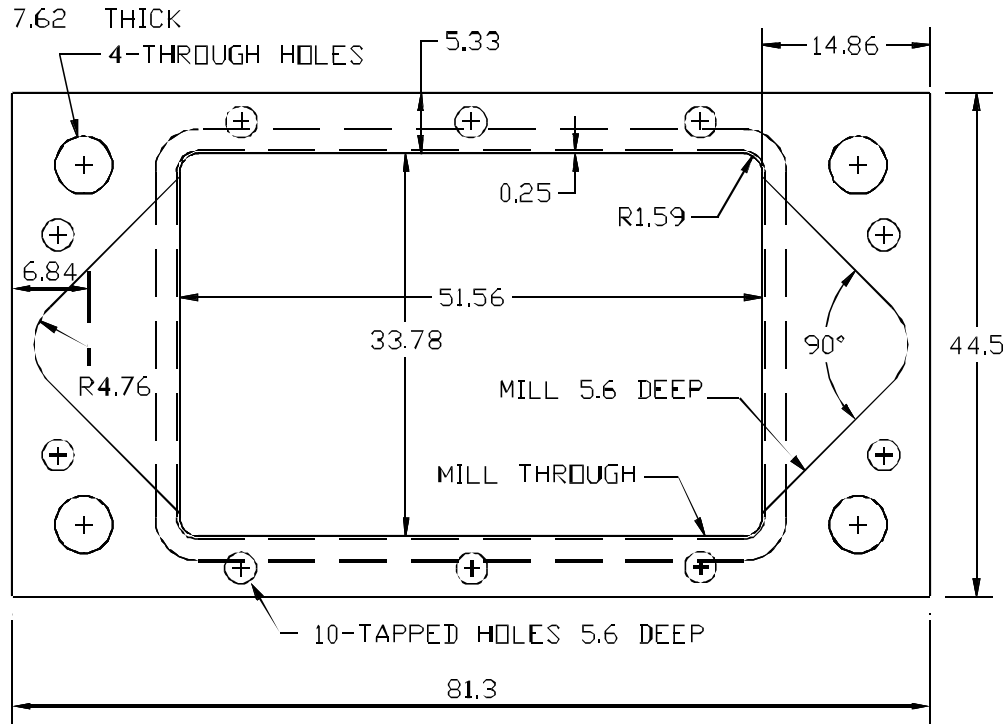
Figure 3.3   Fin array housing (dimensions in mm).

PAO fluid (a non-toxic and nonflammable synthetic oil) was used as the coolant. The thermophysical properties of PAO is listed in Table 2. The coolant flow was circulated by a magnetic gear pump at flow rates up to 0.126 L/s (2.0 gpm). The coolant flowed downwards int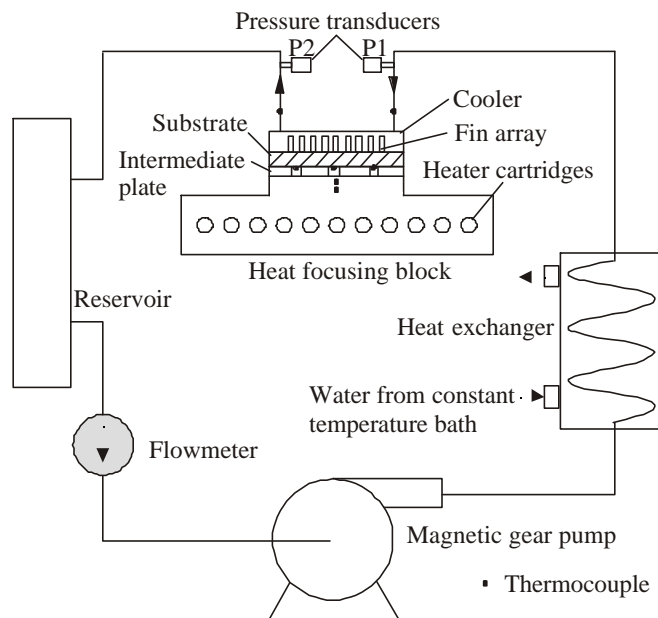o the cooler, turned 90º to the fin channels, crossed the fin array, and left the cooler at right angles to the substrate. The coolant flow rate was regulated by a pump control system and measured using a turbine flow meter operating with a signal conditioner. The pressures at the inlet and outlet of the cooler were measured using two pressure sensors. The coolant temperatures at the inlet and outlet of the cooler were measured using two probe thermocouples. The inlet coolant temperature was regulated by the constant temperature bath that supplied cooling water to and from the fin array cooler. The mean temperature of the coolant through the cooler, $T_{l,m}$, was an arithmetic average of the coolant temperatures at the inlet and outlet of the cooler. Coolant properties were predicted at the mean temperature of the coolant.

11

Table 2   Thermophysical properties of polyalphaolefin (PAO)

Temperature K (Kelvin)	Density kg/m^3	Dynamic viscosity kg/m*s	Specific heat kJ/(kg*K)	Thermal conductivity W/(m*K)
219	860	1.032	1.74	0.152
239	841	0.24	1.94	0.149
259	823	0.041	2.07	0.147
279	806	0.0124	2.17	0.144
299	789	0.0054	2.23	0.142
319	772	0.0033	2.28	0.140
339	754	0.0022	2.33	0.138
359	736	0.0015	2.40	0.136
379	717	0.0011	2.50	0.134
399	697	0.0010	2.65	0.132
419	676	0.000541	2.85	0.130

A heat focusing block made of copper with inserted cartridge heaters was used as heat source. A DC power supply unit was used to provide power for the cartridge resistors. Eight thermocouples were embedded in 0.7 mm holes drilled along two planes in the upper part of the heat focusing block, forming four pairs of thermocouples. The distance between two thermocouples in each pair was 5.1 mm. The heat rate, Q, was calculated using average temperature difference between the two planes where the thermocouples were located, using the distance between the two planes and using the contact area of the intermediate plate. The heater and the cooler were well insulated with fiberfrax.

Ten thermocouples were used to measure the temperatures on the bottom substrate surface. To protect the thermocouples against a contact with the heater, an intermediate plate with ten slots was soldered onto the substrate. The thickness of the intermediate plate was 0.8 mm. The thermocouples were inserted into the slots and soldered onto the substrate wall. The thermocouple bead diameter was

0.3 mm, smaller than the slot width of 0.5 mm. Epoxy was filled in the thermocouple slots to insulate the thermocouple from the heater. The substrate with the intermediate plate was sandwiched between the fin array housing and the heater. The intermediate plate was tightly attached to the heater surface by a compression assembly. Thermal grease was used to minimize the thermal resistance between the intermediate plate and the heater. The thermocouple locations are shown in Figure 3.4. The mean temperature on the bottom surface of the substrate, $T_{s,m}$, referred to an arithmetic average of all the temperatures indicated by the thermocouples on the bottom surface of the substrate. The average temperature on the substrate upper surface (on the flow side), $T_{b,m}$, was calculated by

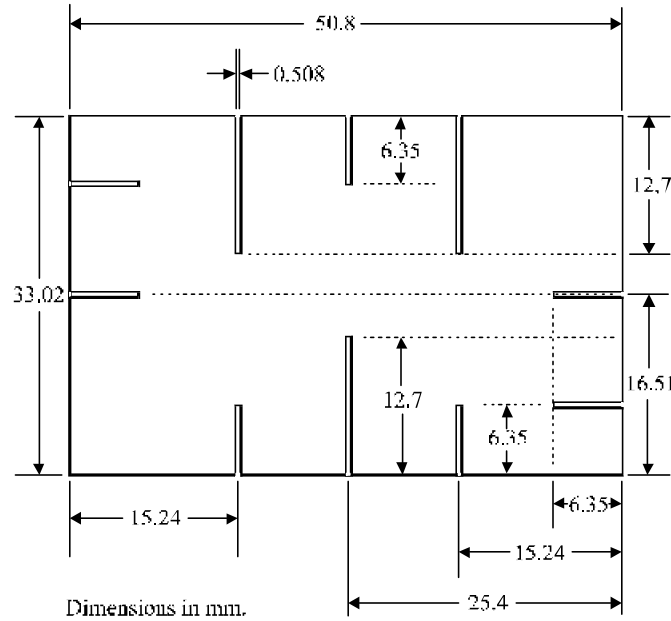$$T_{b,m} = T_{s,m} - \frac{qt_s}{k_s}. \tag{1}$$

Figure 3.4   Intermediate plate and thermocouple locations on the substrate.

13

During the test, the experimental conditions were varied in the following range:

Input power   150 W to 870 W

Coolant flow rate   0.033 L/s (0.52 gpm) to 0.126 L/s (2 gpm)

Coolant inlet temperature   30°C to 75°C.

The coolant inlet temperature of 75°C was usually employed for designing electronic cooling devices on board aircraft.

4   MEASUREMENT UNCERTAINTY

A Hewlett Packard 3852A data acquisition system was used to make all temperature measurements. This device has a resolution of 0.02°C. The data acquisition unit and type T thermocouples were compared to a precision digital resistance temperature device with 0.03°C rated accuracy. The system accuracy was found to be within 0.2°C over the range of interest. In the steady state, the thermocouples fluctuated within 0.2°C.

The accuracy of the distance between two thermocouples in each pair in the heater was within 0.3 mm. The uncertainty of the pressure measurements was 6.9×10^{-3} bar. The turbine flow meter was calibrated for PAO fluid. The uncertainty of the turbine flow meter was 1.9×10^{-3} L/s.

All of the experimental data such as the temperatures, the input power and the coolant flow rates were acquired 50 times in an interval of 1 minute and the average values were recorded after a steady state was reached.

5   RESULTS AND DISCUSSION

Experimental results were obtained for a range of heat rates from 7 to 47 W/cm^2 with reference to the heating area, A_h. The Reynolds number variation was from 53 to 482. It was noticed that the pressure drops across the cooler were smaller than 0.02 bar under the present conditions. The heat transfer coefficient was implicitly expressed by the following equation [12]:

$$Q = [n_f n_{st} \sqrt{hPk_f A_c} \tanh(sl_1) + A_b h](T_{b,m} - T_{l,m}), \tag{2}$$

where

$$s = \sqrt{\frac{hP}{k_f A_c}}. \tag{3}$$

The heat transfer coefficient, h, was iteratively computed from Eqn.(2) using the experimental data.

Experimental data of heat transfer were expressed as $Nu/Pr^{1/3}$ versus Re. They are shown in Figure 5.1 for the offset fin strip layout and in Figure 5.2 for the aligned fin strip layout, with different fin strip gaps. In Figure 5.1, a correlation by Wieting for offset strip fin (without fin strip gaps) [4] is presented for comparison. In the range of Re $\leq$ 1000, Wieting's correlation was expressed as [4]

$$Nu = 0.483 \left(\frac{l}{D_h}\right)^{-0.162} \left(\frac{b}{a}\right)^{-0.184} Re^{0.464} Pr^{1/3}, \tag{4}$$

where

$$Nu = \frac{hD_h}{k_l} \tag{5}$$

$$Re = \frac{ruD_h}{m} \tag{6}$$

and

$$D_h = \frac{2ab}{(a+b)}. \tag{7}$$

It may be seen from Figure 5.1 that the value of $Nu/Pr^{1/3}$ increases with an increase in Re. The experimental relations between $Nu/Pr^{1/3}$ and Re are close to each other for different fin strip gaps smaller than 0.38 mm. The values of $Nu/Pr^{1/3}$ are noticeably greater for $l_g = 1.0$ mm than for $l_g \leq 0.38$ mm. This implies that as it is increased above a certain value, the fin strip gap for the offset fin strip layout helps to rebuild thermal boundary layer adjacent to the fin surfaces downstream from the leading edge of the separated fin strips and consequently increases the heat transfer coefficient. It is exhibited that Wieting's correlation is close to the cases for $l_g \leq 0.38$ mm.

Figure 5.2 shows also the increase in $Nu/Pr^{1/3}$ value with an increase in Re for the aligned fin strip layout. However, for the aligned fin strip layout, the value of $Nu/Pr^{1/3}$ increases with every increment of l_g . In this case, contribution of the fin strip gap to enhancing the heat transfer coefficient is more noticeable because larger leading edge areas of the plain fins are exposed to the bulk flow.

Figure 5.3 shows an effect of mass flow rate on the substrate-to-coolant temperature difference at the inlet coolant temperature of 74.5°C for the offset fin strip layout with $l_g = 0.13$ mm. For a given heat flux rate, the substrate-to-coolant temperature difference decreases with an increase in the mass flow rate. It is shown that for mass flow rates greater than 0.077 kg/s, the cooler can transport heat at the heat flux level of 46 W/cm^2 at substrate-to-coolant temperature differences smaller than 37.5°C. Generally for applications to electronics cooling, the expected value of $(T_{b,m}-T_{l,m})$ should be smaller than 40°C.
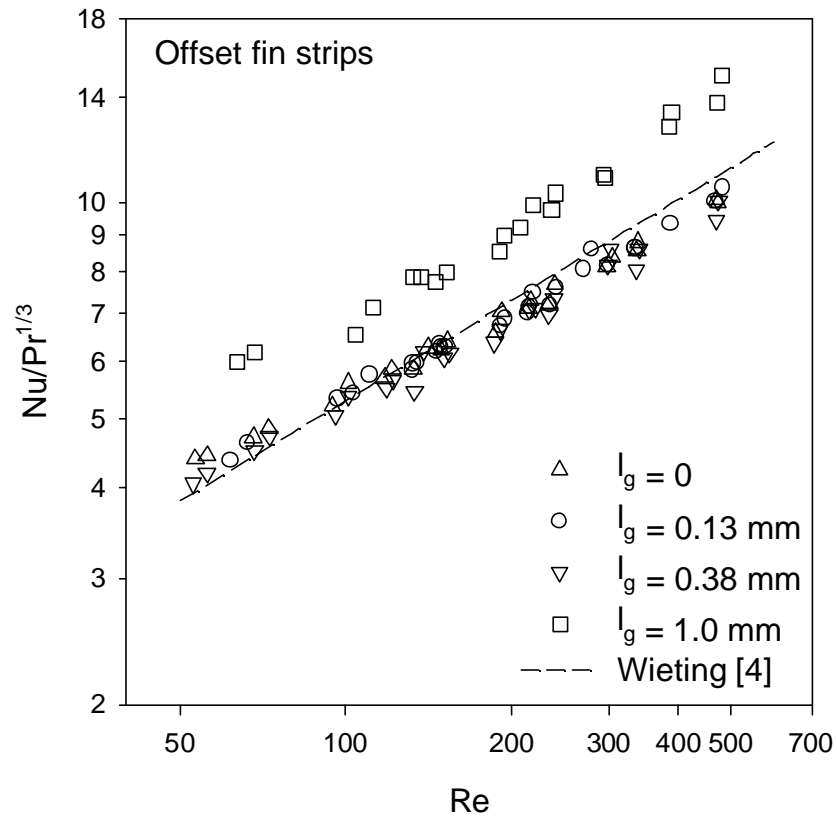
Figure 5.1 $Nu/Pr^{1/3}$ versus Re for the offset fin strip layout with different fin gaps and Wieting's correlation [4].
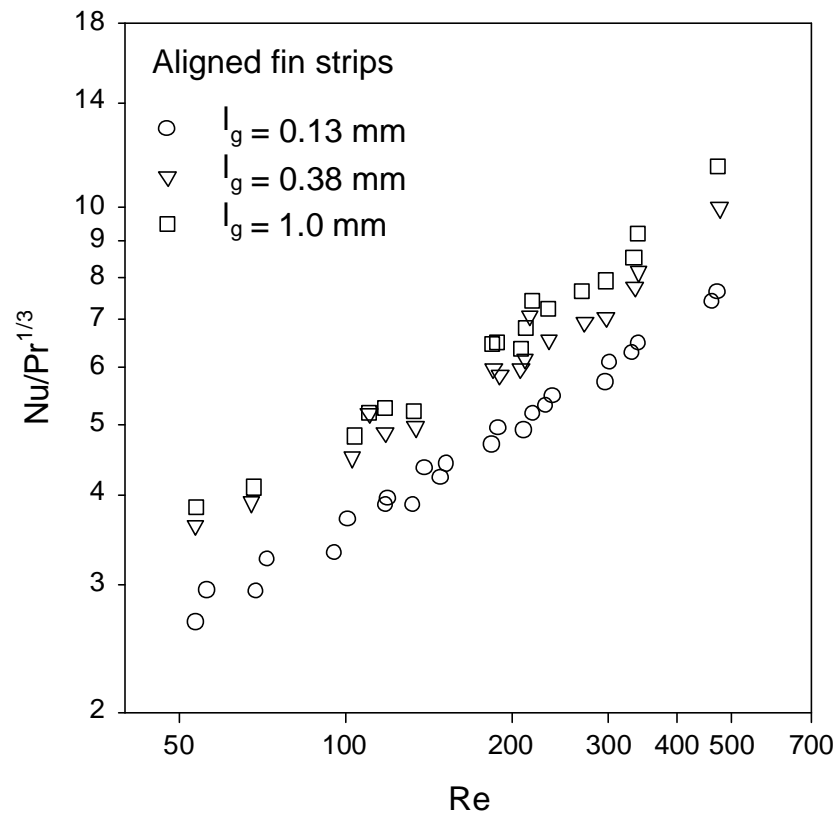
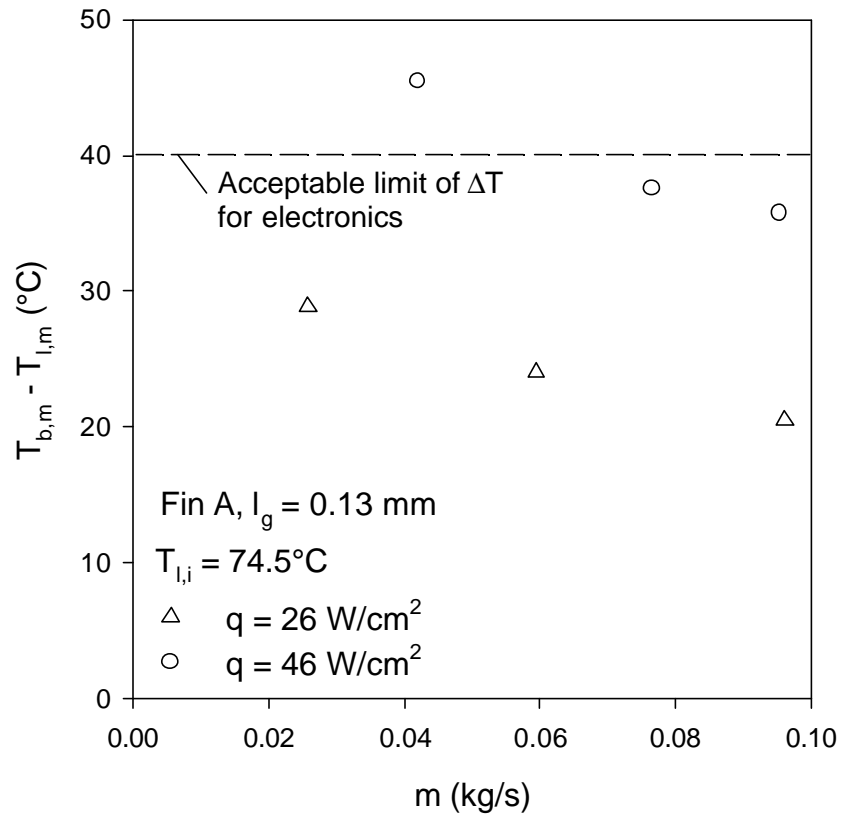Figure 5.2 Nu/Pr$^{1/3}$ versus Re for the aligned fin strip layout with different fin gaps.

Figure 5.3   Substrate-to-coolant temperature difference versus mass flow rate.

6   HEAT TRANSFER CORRELATION

It may be noted from Figure 5.1 and Figure 5.2 that the relation of $Nu/Pr^{1/3}$ with Re follows the power-law. To consider the effect of the fin strip gap, a dimensionless variable of $(1+l_{eff}/t)$ was introduced where l_{eff} was the effective fin strip gap above which l_g would influence the heat transfer coefficient. The ratio of l_{eff} to t (fin thickness) was regarded as the measure of exposing the fin leading edge to the bulk flow. To include the above mentioned variables, the correlations for the offset and aligned fin strip layouts were developed as follows:

For the offset fin strip layout:

$$Nu = 0.8217 \, Re^{0.405} \, Pr^{1/3} \left(1 + \frac{l_{eff}}{t}\right)^{0.258} , \tag{8}$$

where

$$l_{eff} = \begin{bmatrix} 0, & l_g \le l_0 \\ l_g - l_0, & l_g > l_0 \end{bmatrix}$$

Where $l_0 = 0.38$ mm.

For the aligned fin strip layout:

$$Nu = 0.3895 \, Re^{0.468} \, Pr^{1/3} \left(1 + \frac{l_{eff}}{t}\right)^{0.283} , \tag{9}$$

where

$$l_{eff} = l_g .$$

It should be pointed out that for $l_{eff} \le 0.38$ mm, correlation (8) is reduced to the case of offset strip fin with all the fin strips connected. The experimental data for the offset and aligned fin strip layouts are compared with Eqn.(8) and Eqn.(9) in Figure 6.1. The correlations fit the data to within mean errors of 3.7% for the offset fin strip layout and 6.6% for the aligned fin strip layout. As seen from Figure 6.1, most of the data fall within ±10% of the corresponding correlations for the offset and aligned fin strip layouts. In general, the heat transfer coefficients are 29% to 36% higher for the offset fin strip layout
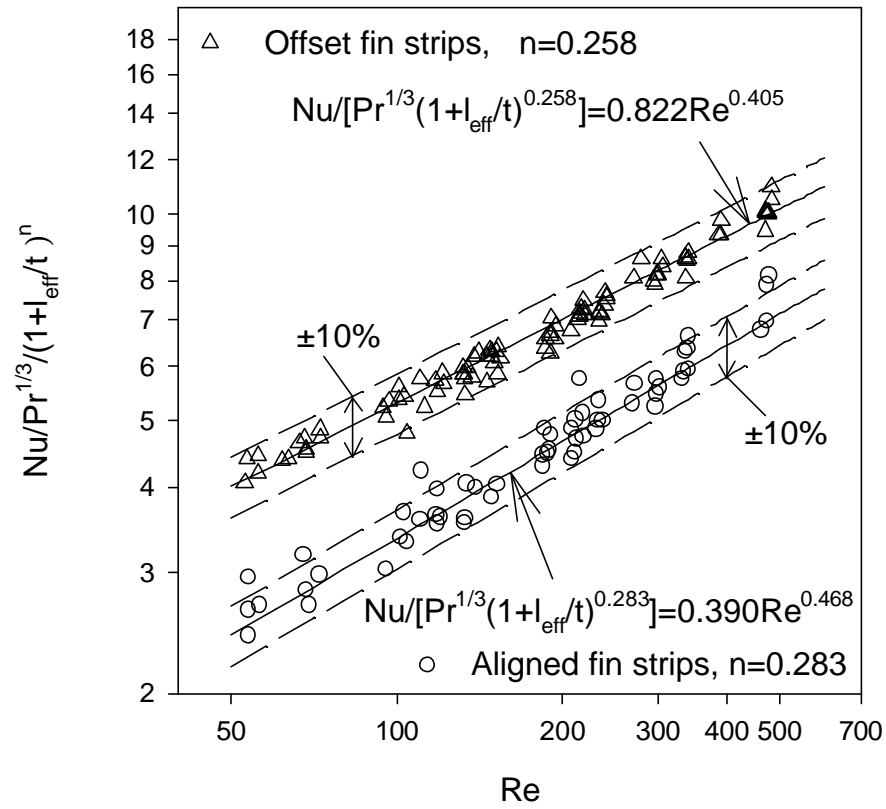
than for the aligned fin strip layout.

Figure 6.1   Comparisons of data for Fin A and Fin B with Eqn. (8) and Eqn. (9).

7   CONCLUSIONS

Conclusions of the present investigation are summarized as follows.

♦ Two new types of plain fin arrays formed by offset fin strips and aligned fin strips have been developed in order to mitigate the thermal stress problem found in the integral finned substrate. A cooler for electronics cooling has been designed using these plain fin arrays.

♦ New heat transfer correlations have been obtained for the plain fin array coolers with the offset fin strip layout and with the aligned fin strip layout. The mean absolute error is 3.7% for the former correlation and 6.6% for the latter. The new correlations reflect the variation of the fin strip gap.

♦ In the present Reynolds number range, the correlation by Wieting [4] approximately predicts the current results for the offset fin strip layout with the fin strip gaps smaller than 0.38 mm.

♦ For mass flow rates greater than 0.077 kg/s, the cooler with the offset fin strip layout can transport heat at the heat flux level of 46 W/cm^2 at substrate-to-coolant temperature differences smaller than 37.5°C.

♦ In general, the heat transfer coefficients are 29% to 36% higher for the offset fin strip layout than for the aligned fin strip layout.

8   RECOMMENDATIONS

♦ Other fluids such as JP fuels and fluorocarbon fluids can be used for test.

♦ Comparison of the present data with data of carbon foam coolers can be made.

♦ Numerical simulation of the thermal performance will be helpful for the understanding of the heat transfer characteristics of the plain fin array coolers.

9   REFERENCES

[1]   Kays, W. M., and London, A. L., "Compact Heat Exchangers," 3rd edn. McGraw-Hill, New York, 1984.

[2]   Shah, R. K., "Compact Heat Exchangers," in *Handbook of Heat Transfer Application,* Rohsenow, W. M., et al., Eds., McGraw-Hill, New York, 1985, pp. 4·174 - 4·312.

[3]   Manglik, R. M., and Bergles, A. E., "The Thermal-Hydraulic Design of the Rectangular Offset-Strip-Fin Compact Heat Exchanger," in *Compact Heat Exchangers*, Shah, R. K, et al., Eds., Hemisphere, New York, 1990, pp. 123-149.

[4]   Wieting, A. R., "Empirical Correlations for Heat Transfer and Flow Friction Characteristics of Rectangular Offset-Fin Plate-Fin Heat Exchangers," ASME Journal of Heat Transfer, Vol. 97, 1975, pp. 488-490.

[5]   Joshi, H. M., and Webb, R. L., "Heat Transfer and Friction in the Offset Strip-Fin Heat Exchanger," International Journal of Heat and Mass Transfer, Vol. 30, 1987, pp. 69-83.

[6]   DeJong, N. C., and Jacobi, A. M., "An Experimental Study of Flow and Heat Transfer in Parallel-Plate Arrays: Local, Row-by-Row and Surface Average Behavior," International Journal of Heat and Mass Transfer, Vol. 40, 1997, pp. 1365-1378.

[7]   Timoshenko, S. P., "Analysis of Bi-Metal Thermostats," Journal of the Optical Society of America, Vol. 11, 1925, pp. 233-255.

[8]   Chen, W. T., and Nelson, C. W., "Thermal Stress in Bonded Joints," IBM Journal of Research and Development, Vol. 23, 1979, pp. 179-188.

[9]   Suhir, E., "Interfacial Stresses in Bimetal Thermostats," ASME Journal of Applied Mechanics, Vol. 56, 1989, pp. 595-600.

[10]   Jiang, Z. Q., Huang, Y., and Chandra, A., "Thermal stresses in Layered Electronic Assemblies," Journal of Electronic Packaging, Vol. 119, 1997, pp. 127-132.

[11]   Watari, K., and Shinde, S. L., "High Thermal Conductivity Materials," MRS Bulletin, June 2001, pp. 440-441.

[12]   Incropera, F., and DeWitt, D. P., "Fundamentals of Heat and Mass Transfer," 4th Edition, John Willey & Sons, New York, 1996.

APPENDIX A: FREE-BODY DIAGRAM OF A LAYERED ASSEMBLY
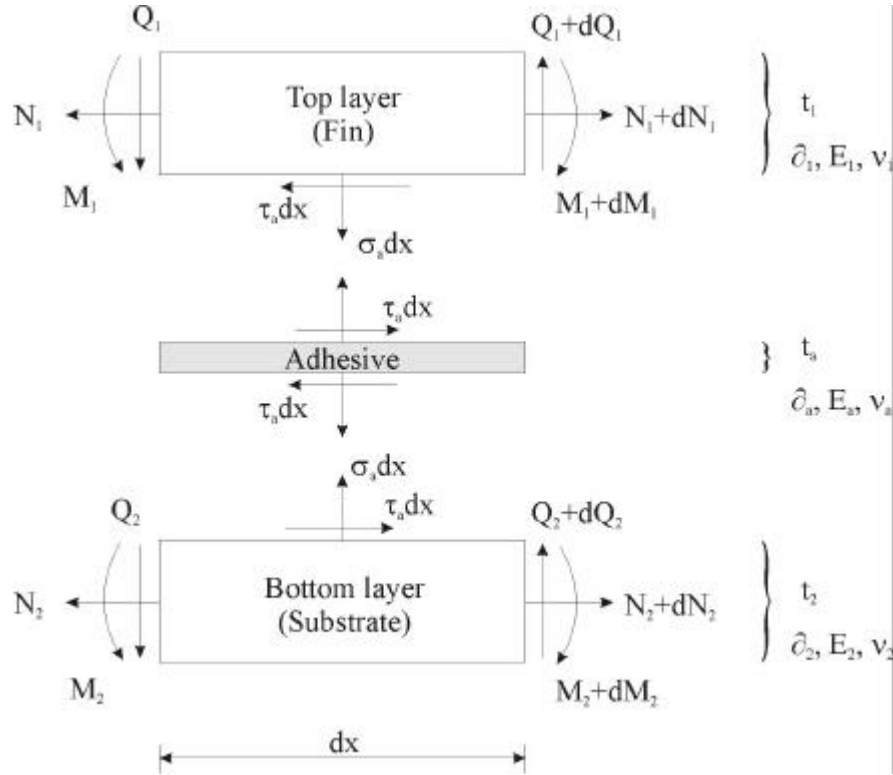
where

E   modulus of elasticity

M   moment per unit width

N   axial force per unit width

Q   shear per unit width

t   layer thickness

α coefficient of thermal expansion

ν Poisson's ratio

σ peeling stress

τ interfacial shear stress

APPENDIX B: UNITARY FIN ARRAY

A rectangular copper sheet can be used to form the unitary fin array. The copper sheet includes several rectangular holes. It is pressed into a die in the transverse direction, forming the corrugated fin strips lining up with each other, and then pressed into another die in the flow (longitudinal) direction, forming the unitary fin array with the expansion turns.
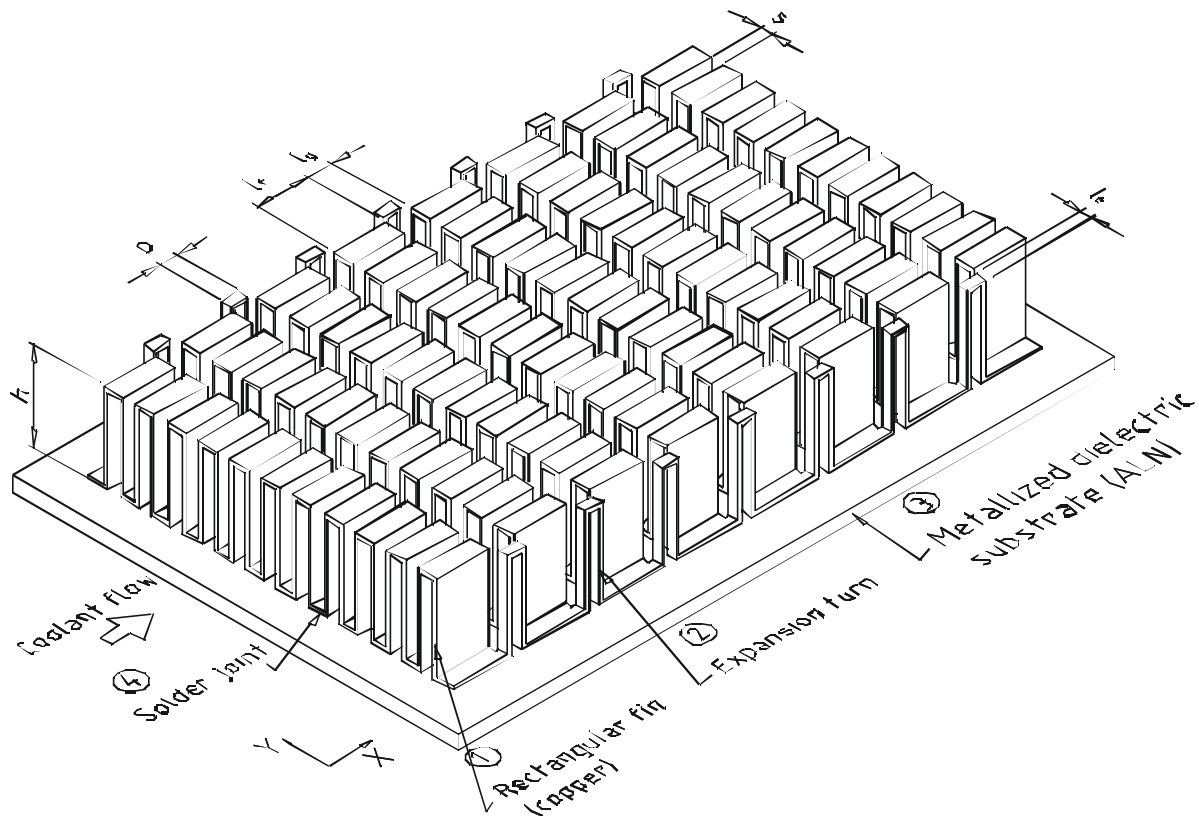
Figure B.1   Unitary fin array with expansion turns.